Column Supported, Irregular Flat Plates with Surface Oriented Moment Distribution

By Kolbjorn Saether, [1]

Abstract

A general flat plate analysis is presented using a development referred to as the Structural Membrane Approach (SMA). This approach is based on a unique structural model which allows slab moments to be represented as a combination of three basic 3-D functions for local moment fields. These functions are referred to as Structural Membrane shapes and express the dualism between plate bending moments and the displacement patterns of stretched elastic membranes subjected to lateral loads.

The original formulation of SMA focused on the determination of the fixed-end-moments in flat plate designs. The present paper extends the capabilities of the SMA by developing a moment balancing between different areas and supports by utilizing a surface oriented moment distribution. This approach results in an extremely efficient, intuitive and useful methodology for analyzing regular and irregular slab layouts.

Introduction

SMA is the dualism between bending moment distributions in flat plates and the deflection of laterally continuously supported regular and irregular slabs to be analytically determined. A central feature of the SMA is the dualism between bending moment distributions in flat plates and the deflection of laterally loaded, elastic membranes (Saether, 1961). This relationship follows from the 4th-order Kirchhoff governing equation for plate bending given by

$$\frac{\partial^4 w}{\partial^4 x} + 2\frac{\partial^4 w}{\partial^2 x \partial^2 y} + \frac{\partial^4 w}{\partial^4 y} = \frac{q}{D} \qquad (1)$$

CE Database subject headings: Moments, Bending Moments, Moment Distribution, Columns, Column Supports, Irregular Flat Plates

---

1 Principal and Chief Engineer, Kolbjorn Saether & Associates, Inc.
1062 W. Chicago Avenue, Chicago, Illinois
E-mail: dovre1@aol.com

which may be decomposed into two membrane-type 2nd order equations. These equations describe the moment and the displacement fields of the plate by the following equations (see Timoshenko, 1959):

$$\frac{\delta^2 M}{\delta x^2} + \frac{\delta^2 M}{\delta y^2} = -q \tag{2}$$

$$\frac{\delta^2 w}{\delta x^2} + \frac{\delta^2 w}{\delta y^2} = -\frac{M}{D} \tag{3}$$

where M is a combined moment defined by:

$$M = \left(M_x + M_y\right)/\left(1 + \nu\right) \tag{4}$$

Equations (2) and (3) are both of the same kind as that obtained for the deflections of a uniformly stressed and laterally loaded elastic membrane. Using Equation 2, Saether (1961) demonstrated that the moment fields over a continuously supported flat plate can be represented by a combination of shapes corresponding to Elliptical Domes (ED), Hyperbolic Paraboloids (HP) and Logarithmic Funnels (LF) (See Figures 1, 2 & 3). Because the fields shown in Figures 2 and 3 correspond to these membrane deflections and as such represent bending moment distributions over slab structures, they are referred to as Structural Membrane (SM) shapes. The equations for these shapes are given by

$$Z_{ED} = k_1 (x^2 + y^2) \tag{5a}$$

$$Z_{HP} = k_2 (x^2 - y^2) \tag{5b}$$

$$Z_{LF} = k_3 \, \mathrm{Log}(x^2 + y^2) \tag{5c}$$

where k_i are constants.

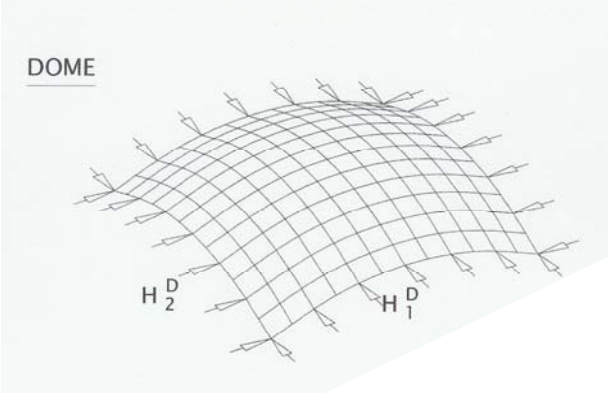

Figure 1. Ellipsoidal dome (ED) geometry

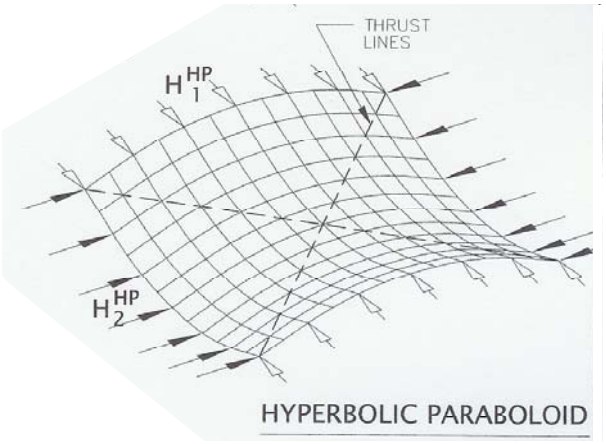

Figure 2. Hyperbolic paraboloid (HP) geometry.

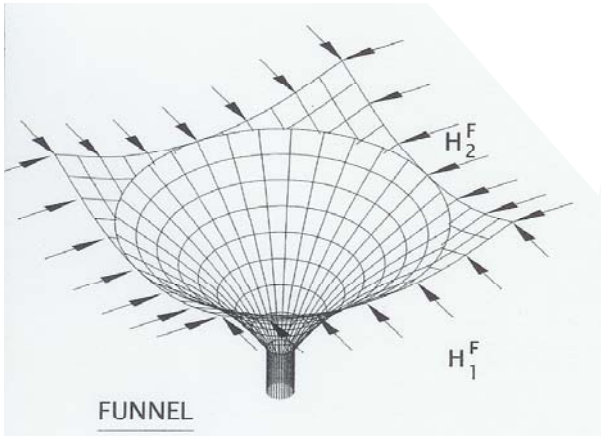

Figure 3. Logarithmic funnel (LF) geometry.

When using the SM model in the analysis of plate bending, the SMA methodology assumes, up front that the Poisons' ratio ν and the twisting moments and shears, M_{xy}, M_{yx}, V_{xy}, $V_{yx,}$ are all equal to zero.

The SMA shares great similarities with the plate analysis approach developed by Marcus (1932) who used a superposition of non-interacting orthogonal fibers in a 'weave' as differential element to represent plate response under applied loads. His derivation of a Cartesian weave led to a moment field that corresponds to the ellipsoidal dome in the SMA and, using a polar weave composed of circular and radial fibers over plate supports, led to a logarithmic expression for support moments. Marcus's work was limited, however, by not addressing the issue of continuously supported plates. This issue is central to the SMA and requires the introduction of the additional moment field given by

the hyperbolic paraboloid. With this addition, the SMA develops a systematic procedure determining the location and transition between the various SM shapes.

It is of interest to note that for membrane continuity the LF corners consist of inverted domes (See Figure 3). In order to carry the imposed load q, these corner units are assumed to contain radial ribs and concentric circles matching the LF. The thrust along the upper rim matches those of the HP and the thrust in at the lower rim matches the increased thrust in the LF.

Saether (1994) pointed out that by combining these equations using the SM model described above, the moments in a flat plate are completely described with a few simple mathematical expressions. (See Figures 2 & 3)

SMA has been favorably compared to methods such as the ACT-318 Direct Design and the Equivalent Frame methods (Saether 1994) The SMA has additionally been compared by Baskaran (2004) to the Finite Element Method, the Yield-Line Approach, the Strip Methods, as well as the Triangle Slab Element Approach. He found the SMA in many respects to be superior to these other methods. SMA provides immediate results such as peak moments and average moments at columns, complete moments throughout the slab and accurate column reactions for uniformly distributed as well as concentrated loads. Furthermore, it provides in one set of calculations the final bi-axial bending in the supporting columns.

Of the many existing analytical and numerical approaches, one method, the Strip Method of Hillerborg (1996), shares some similarity with the SMA in that the slab is analyzed as a network of column and middle strips applicable to regular and irregular slabs. However, the Strip Method is based on determining “hog” and “soft” lines throughout the slab governed by a series of rules that result in a relatively complicated analysis. Compared to this the SMA is based on a systematic, geometric decomposition of the slab into local regions which directly demarcates span lengths and equivalent column and middle strips allowing for the development of a compact methodology for slab analysis.

Finite element methods offer complete versatility in the analysis of structures but, even in specialized commercial finite element codes written for the structural engineering field (Etabs 2005), there are various issues that detract the user in a numerical approach compared to the present analytical model. These deficiencies include the possibility of introducing errors in defining the structural model, failure in obtaining converged solutions over all local regions and difficulties in the reduction and interpretation of the output data. Other difficulties encountered with the use of specialty finite element codes are discussed in reference 9.

When implemented in a computer code, the SMA analysis is accomplished with a small numerical effort that is only a fraction of what is needed using general finite element methods. In addition, SMA is shown in numerous comparisons to be accurate within the ‘error-bands’ that exist when translating an idealized engineered design to the actual

structure. Overall, the SMA method has been found to be versatile, fast, accurate and superior to most other analytical approaches (Baskaran, 2004).

In concrete plate design, it is generally accepted that the predicted peak slab moments near the columns may be reduced to average values when allowing for cracking of the concrete and yielding of the reinforcing steel in these regions. The SMA, in addition to determining the maximum peak moment, directly calculates these average column moments.

In the SMA, the shapes of thin shells and the moments in flat plates can be calculated for column layouts containing regular grids such as equilateral triangular and hexagonal grids and completely irregular support grids. It uses a rigid pattern for defining all moment fields giving the location of the juncture lines of these shapes required to establish the continuity between the SM surfaces. For symmetrical 3-D moment fields, the corresponding contour lines prove to be circles or symmetrical hyperbolas. This is not the case for unsymmetrical layouts where these change into ellipses with complex integrals that need to be evaluated. However, small modifications in the elastic membrane shapes that return these shapes to circles or symmetrical parabolas have been found to cause only minor changes in the corresponding moments. This permits non-symmetrical layouts to be analyzed with the same ease as the symmetrical shapes. These modification are described later in this paper.

The systematic procedure of discretizing the slab layout into specific moment functions is a primary component of the SMA methodology. Within each region of the slab, local coordinates, (x', y'), are defined with the x' axis running along lines connecting adjacent columns and the y' axis is assumed perpendicular to this in a counterclockwise sense. The uniform load q is assumed equally divided in the two orthogonal directions x' and y'.

Local field moments in SMA are computed along both the x' and y' axis. In the SM model, principal moments are given by:

$$M(x) = H(x)*e \quad \text{and} \quad M(y) = H(y)*e \tag{5}$$

Where H are the horizontal thrusts located at the edges of each unit in x and y directions, respectively, (See Figure 3), and are the heights of the SM surface above these thrust lines at this location.

The flexibility of this general SMA approach in the analysis of uniformly and randomly supported slabs is presently extended to compute final support moments. These support moments are obtained from initial fixed-end moments by the application of governing boundary conditions that are enforced along the interior and exterior edges of the various moment areas and subjected to the application of a surface oriented moment distribution. Here the moments are distributed as functions of the relative stiffness within the slab and between the slab and the supporting columns. At the completion of the analysis, all local

moments are transformed into the global coordinate system and summed up to give measures of the global moments M_x and M_y throughout the entire slab. Once these moments have been determined, individual column loads are corrected to account for the effect of the change in the slab moments from the fixed-end-moments to the final moments in the fully elastic system.

In this work, it is shown that the SMA yields comparable results to detailed finite element analyses with significantly less computational efforts. Additionally, representative samples using the SMA have shown the enormous simplification in the moment analysis due to the one a priori selection of assumed field solutions and the rapidly obtained solution for average support moments. This is in contrast to standard finite element solutions that are based on slowly convergent minimum energy principles. The result is an ideal theoretical basis for a rapid and versatile design tool for the analysis and design of regular and irregular slab layouts.

1. SMA Analysis

The first step in the SMA analysis procedure is to establish the specific outlines of the geometric regions over which the various SM shapes of field moments are identified. The determination of these geometric delimiters of the flat slab configuration is an important contribution of the SMA and warrants an extended discussion. Based on a prior understanding of how these moment fields originate, the outline of these regions are determined by identifying geometric quantities referred to as “column-lines” and “thrust-lines”. The geometry of the resulting SM shapes (Shown in Figure 9) is further controlled by quantities referred to as SM parameters. In shell design they are referred to as the “fall-lines of the shell”. As detailed in Saether (1961), circular LF moment areas, are centered over each column, ED areas are located at the center of the interior of the slab entity bounded by column lines, and HP moment areas are centered across intersections of thrust lines. The HP functions in such a way that the LF and ED are seamlessly connected. The HP forms the transition between the LF and ED areas. Details of the construction of these geometric quantities are outlined below.

Column lines in the SMA are the dominating sets of lines connecting adjacent columns. They define the interior span lengths. These are readily identified for rectangular (Figure 7a), equilateral triangular (Figure 7b) and equilateral hexagonal layouts (Figure 7c). For randomly oriented columns the definition of column lines requires some additional considerations (See Figure 7d). In all cases, column lines exist between adjacent exterior columns. For interior columns in an irregular layout, a specific set of rules is required to determine the existence of any connecting column-lines (Figures 7d & 8). These rules will be discussed in more detail later in this section.

The following are steps for determining column-lines, thrust-lines and SM shape outlines for regular SM layouts (See Figures 4, 5 and 6). In each case the mid-point of the intersecting lines is the controlling point for the following set of lines. The mid point of the column-lines identify the location of the thrust-lines, from here the midpoint of the thrust-lines identifying the end-points of the SM shape outlines.

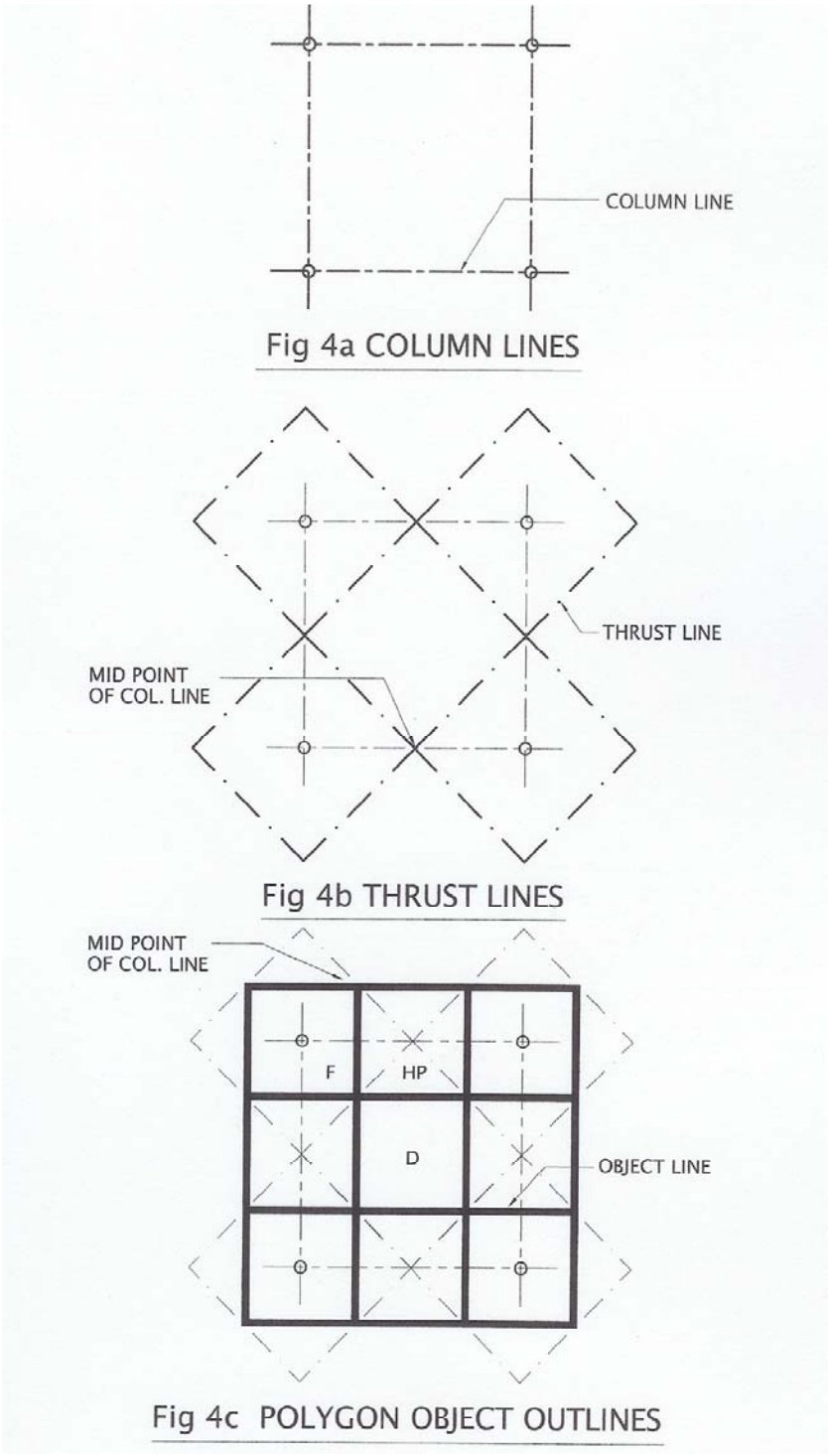

Figure 4. Geometry of rectangular structural membrane layouts.

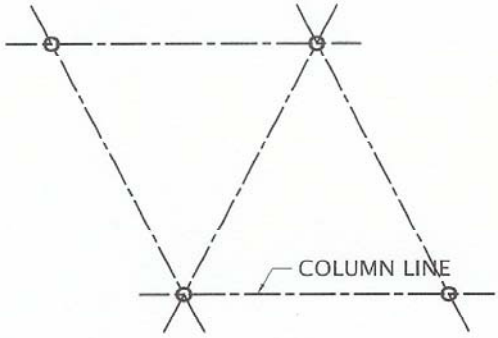

Figure 5a. Column Lines

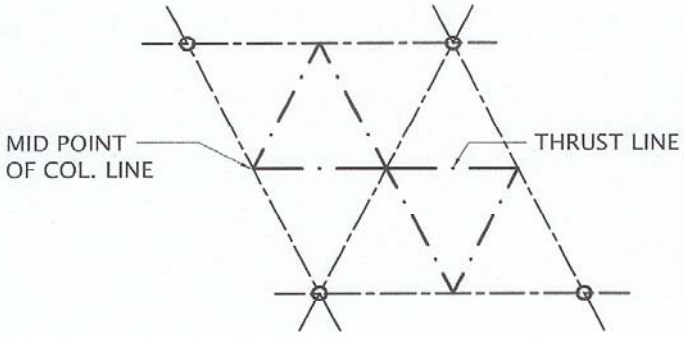

Figure 5b. Thrust Lines

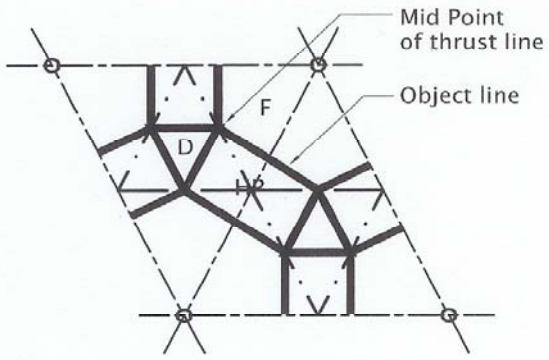

Figure 5c. Object Lines

Figure 5. Geometry of triangular structural membrane layouts.

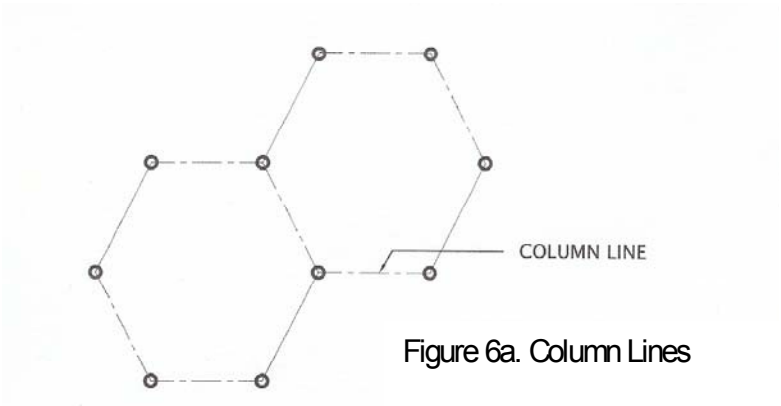

Figure 6a. Column Lines

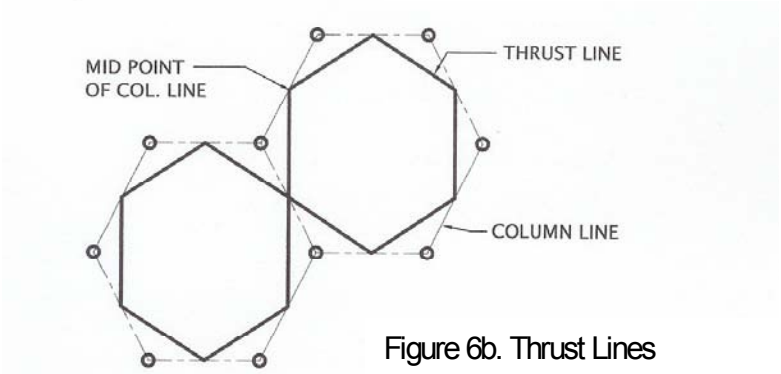

Figure 6b. Thrust Lines

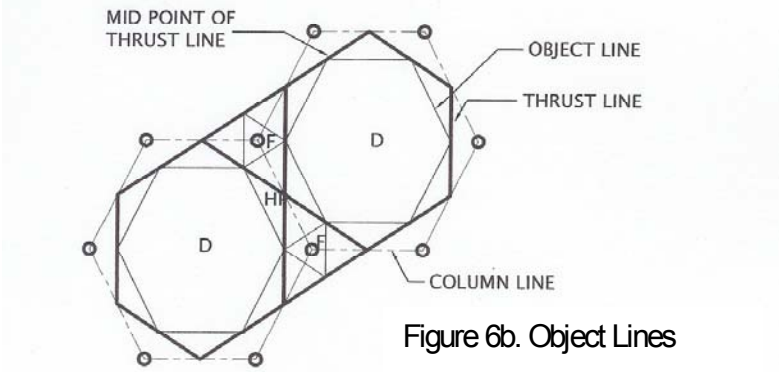

Figure 6b. Object Lines

Figure 6. Geometry of hexagonal structural membrane layouts.

In Figures 7a, 7b and 7c, the resulting floor plans are shown for square, equalateral triangular and hexagonal column layouts. Figure 7d shows a floor plan for an irregular column layout using the SMA rules.

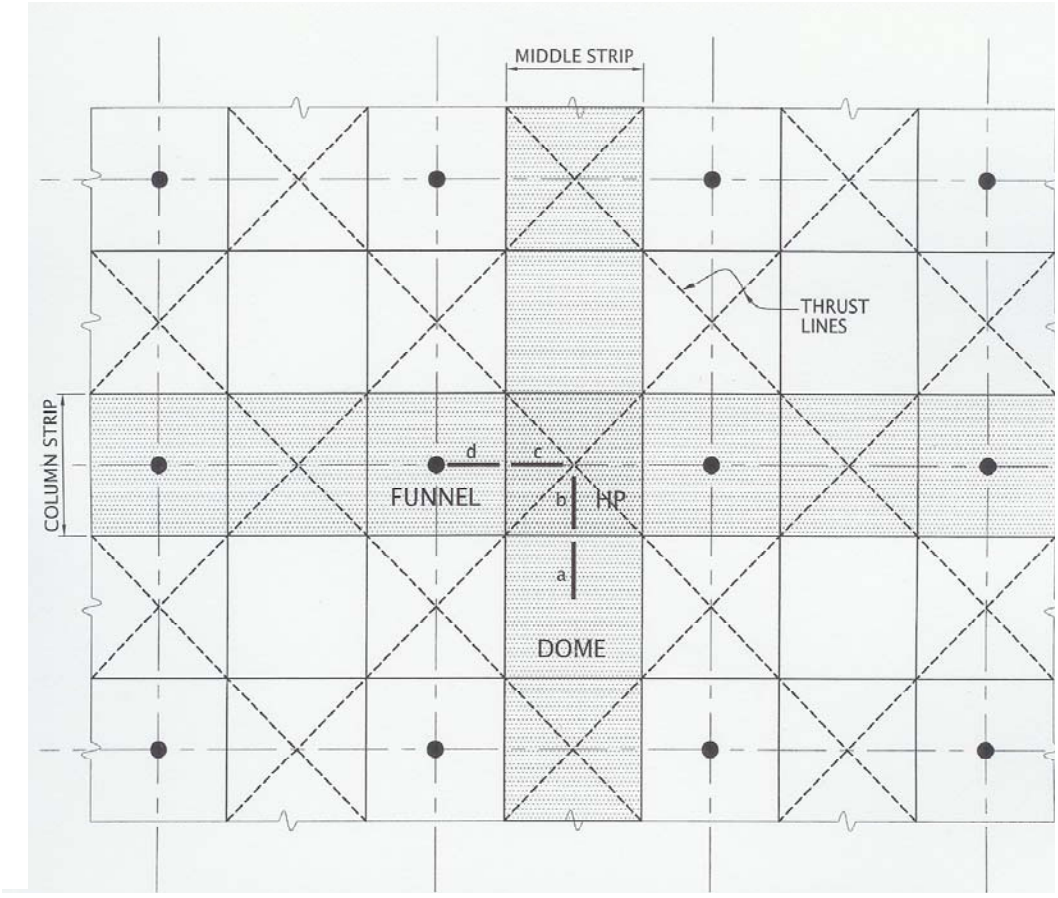

Figure 7a. Structural Membrane configuration developing a square-column plan.

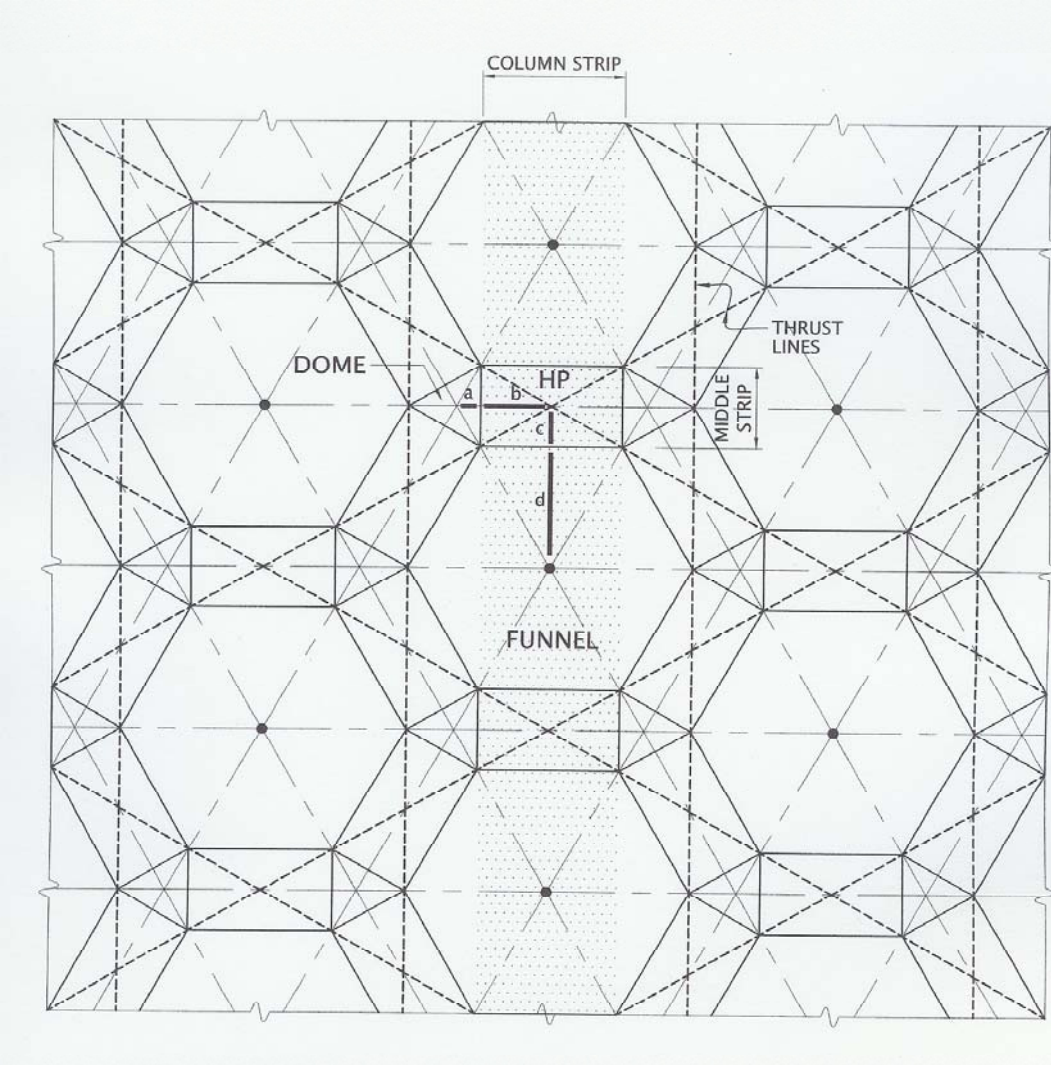

Figure 7b. Structural Membrane configuration developing an equilateral-triangular column plan.

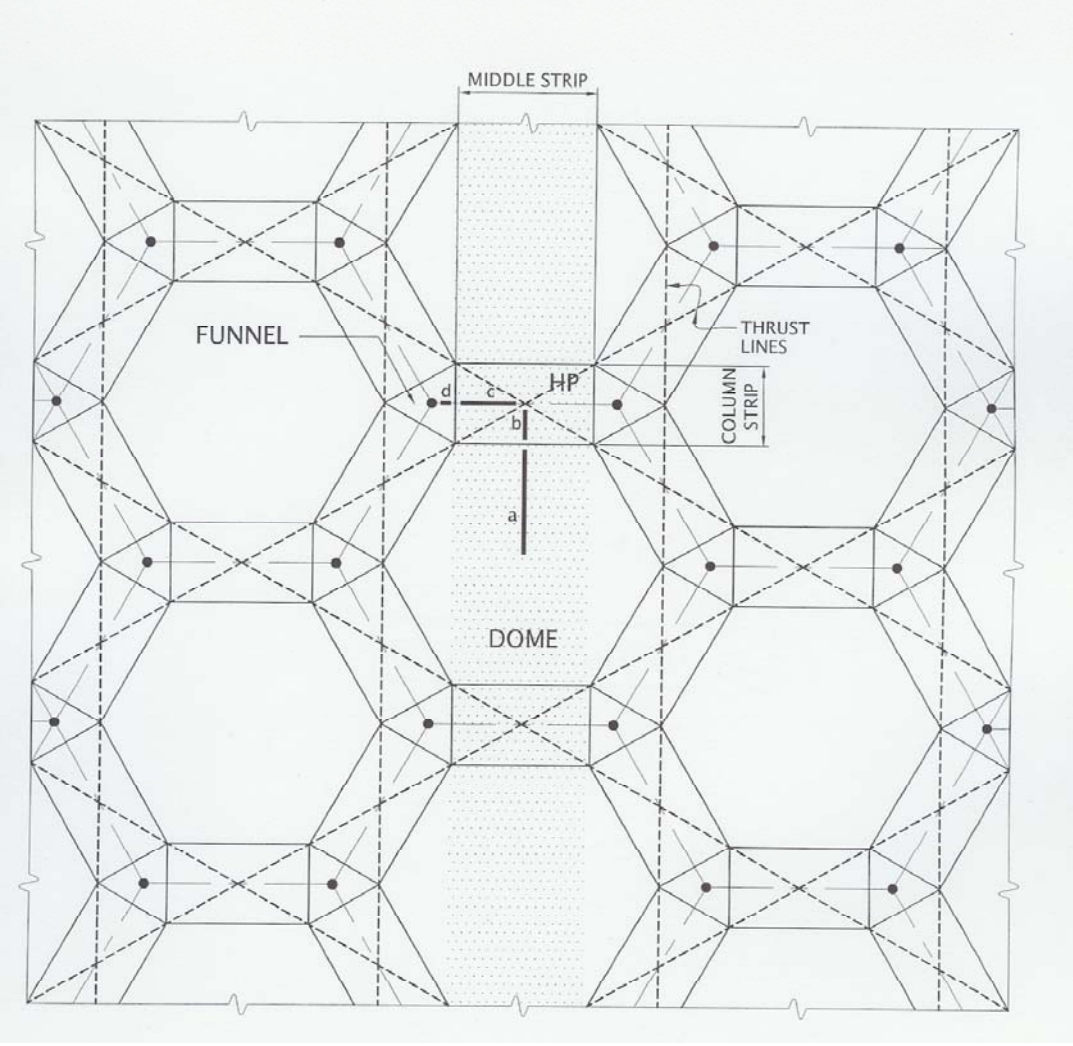

Figure 7c. Structural Membrane configuration developing a hexagonal column plan.

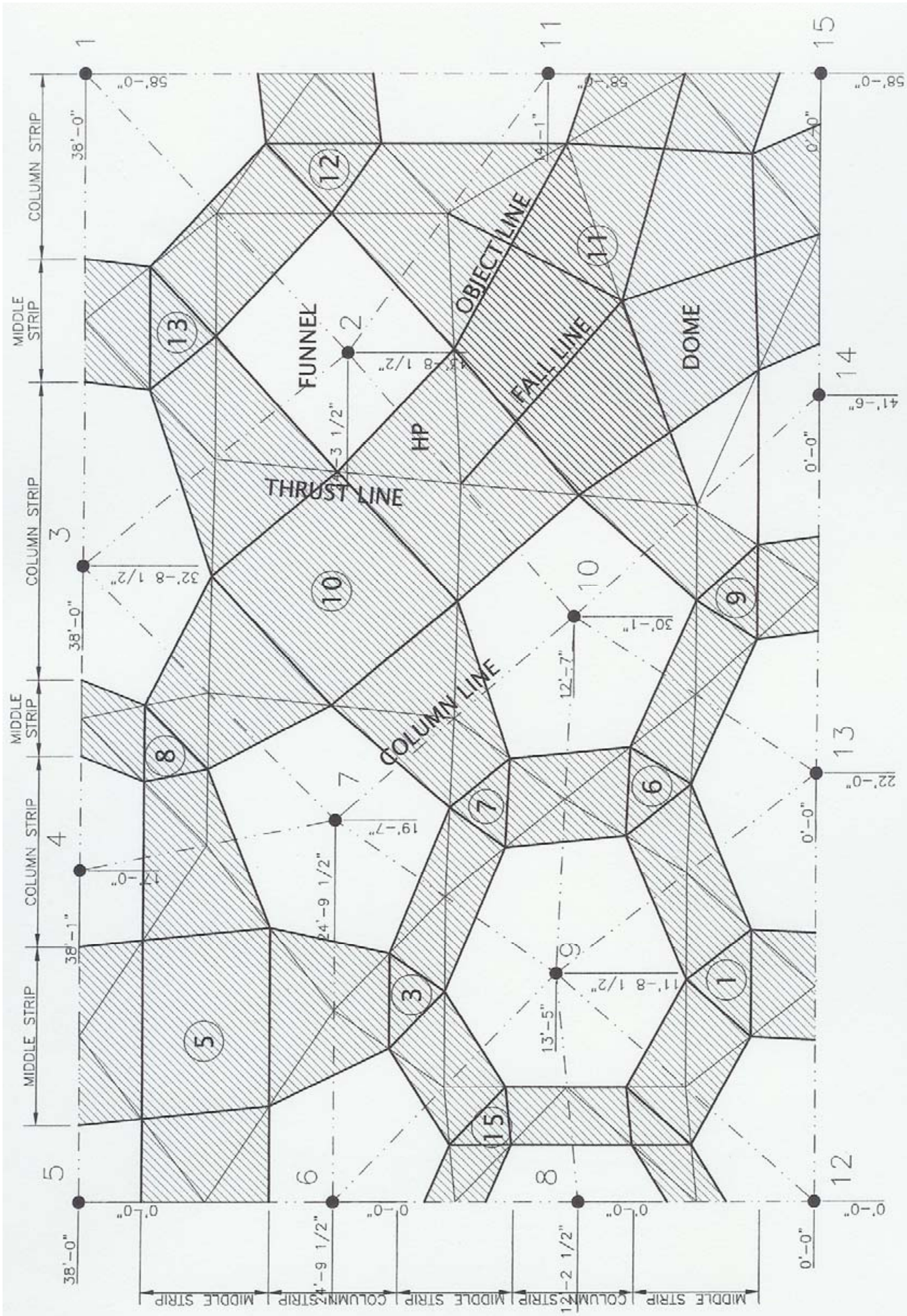

Figure 7d. Typical floor plan with irregularly located columns.

Most existing flat plate design programs pertain to rectangular column layouts. Indeed, regular rectangular layouts are the only slab configurations dealt with in the ACI 318 Direct Design and the Equivalent Frame Methods. The only exception is an allowable 10% offset, in some limited cases an allowable 20% offset of the columns, from the orthogonal layout. For irregular designs, code requirements simply state that "other methods used must be justified by the engineer with regards to equilibrium, geometric compatibility and adequate strength and serviceability including deflections."

The orthogonal arrangement of the columns is important in the operation of converting the unit bending moments expressed in foot-kips per foot into total moment vectors. This is done by calculating the latter as unit moments times the applicable widths and expressed in foot-kips acting along the various column-lines. This operation can be done accurately if adjacent column-lines intersect at 90˚ angles. In this case the two moment directions are independent of each other and the translation from unit moments to total moment vectors is accurate, allowing column-reaction adjustments, carry-over-moments, moment-distributions and moment-balancing to be carried out vectorially with great accuracy.

If the column-lines show skewed or irregular arrangements, however, the calculation of the moment vectors is more involved. When adjacent column-lines are not at 90˚ angle to each other, the unit-moment contributions from these column lines become interdependent. In this case the above listed methods of converting unit moments to total moments have been found by this author to be acceptable approximations for column lines intersecting at angles from 90˚ down to a limit of 35˚. Below this value it is necessary to determine the controlling principal unit moments of the two moment fields using transformation methods such as Mohr's circle, (See Den Hartog, 1952) using average data from the two moment fields. These principal moments are by definition orthogonal and may be used to represent the governing moments in a moment-balancing procedure described in a later section of this paper.

The procedure of determining the governing slab geometry begins with the determination of column lines. Some examples of column line determinations for irregular layouts are given in Figure 8.

The general procedures for designating regions in which particular SM solutions are determined involve certain limiting factors. In the generation of column lines, if the angle between two adjacent potential column-lines in the floor plan layout is less than 70°, a column-line will exist between the ends of these two lines, unless, in the case of quadrilateral areas, the opposite angle is larger than 130^{o}. This corresponds to the before mentioned 35° lower limit. If the initial angle is larger than 70°, no column-line appears between the ends. The angles of 70° and 130° have been found to represent the approximate border between two possible SMA approximations to be used in the analysis, the first using one SM shape and the second using two SM shapes. This transition is depicted in Figure 8 and is used to obtain an optimum in accuracy in representing the local moment fields. One more modification with regards to an angle β will be needed as shown in the following two chapters.

ORIGINAL **FINAL LAYOUT**

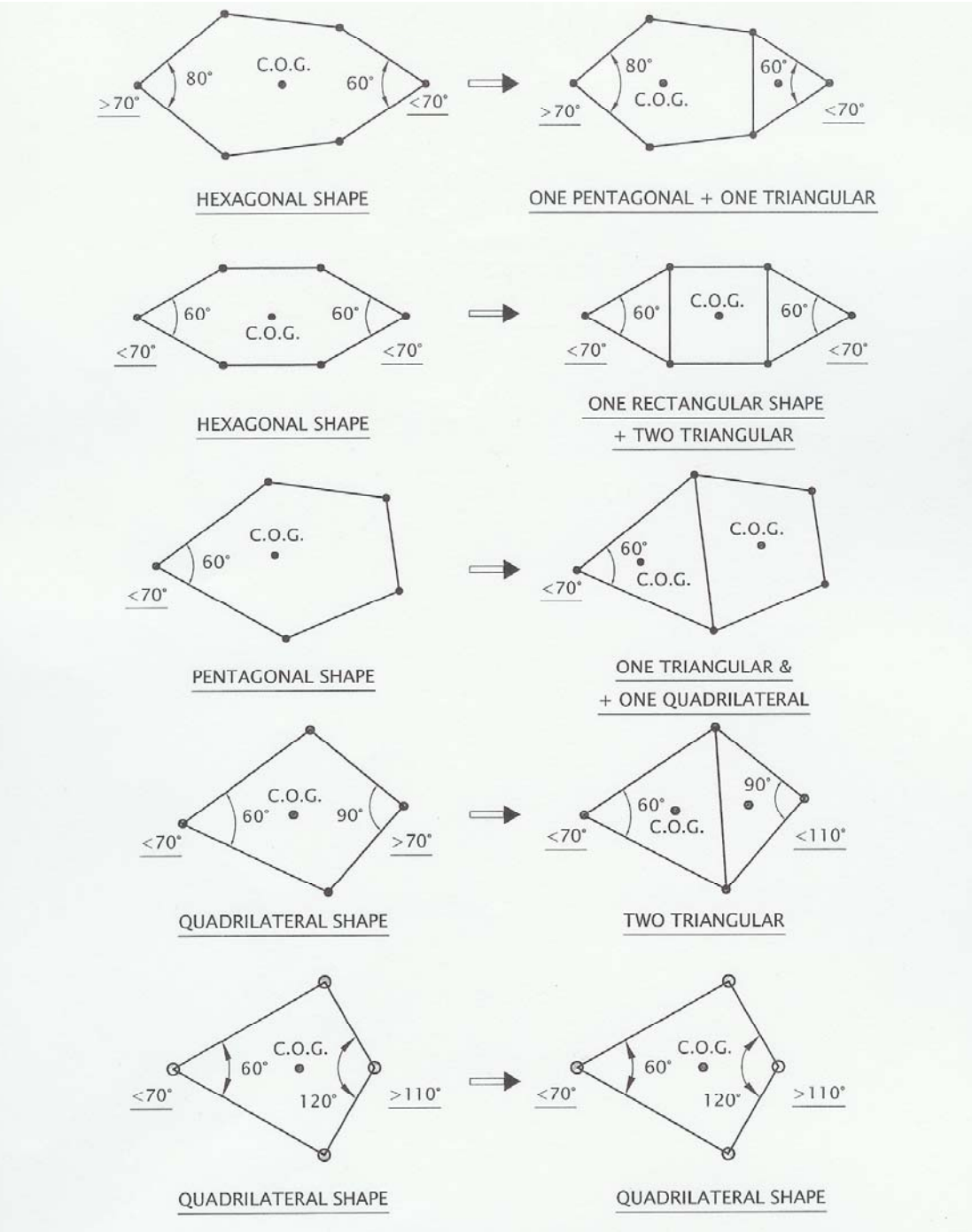

Figure 8. Determination of column lines and basic fields.

The contour-lines describing the deflected membranes in these areas would otherwise consist of skewed, elliptical or dumb-bell shapes, with the consequence that their evaluation would preclude any simple description. When using the limiting angles of 70° and 130° as guide in the determination of the controlling column-lines, and with the next described adjustment of the angle β, the moment intensities are only slightly changed from their true values.

Thrust lines connect the mid-points of any two adjacent column lines as shown in Figure 9 and, in the membrane analogy, are straight line thrust components completely enclosed within the membrane surface. In an actual thin-shell concrete structure these could be straight reinforcing bars or pre-stressing cables required to furnish the required thrust for the equilibrium of the membrane surface. Finally, SM moment area outlines are determined by lines that connect the midpoints of any two adjacent thrust lines The resulting geometric slab regions are shown in Figures 4, 5 and 6. These lines identify the outlines of the basic units of the moment fields. The fall lines are described by a set of parameters, *a*, *b*, *c* and *d,* as shown in Figure 9. These parameters are fundamental to the SMA and are used to calculate the bending moments and column reactions in the slab and supporting columns.

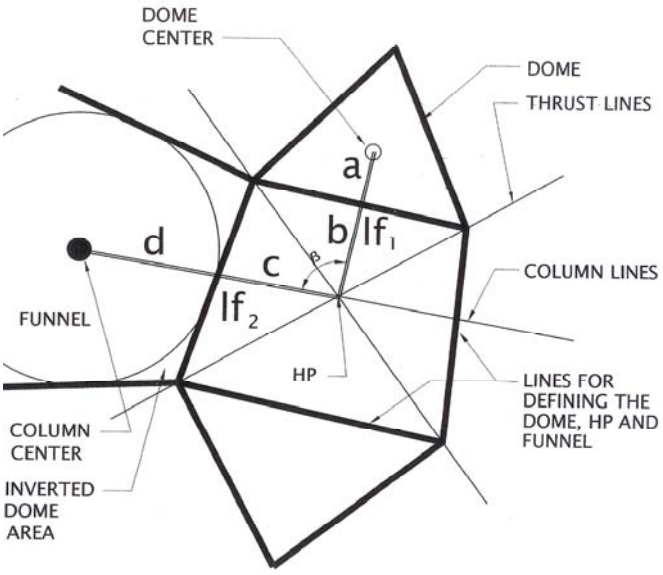

Figure 9. Structural membrane components.

The SM parameters describe the moment field's geometry and have the following values: $Lf_1 = a + b$ and $Lf_2 = c + d$ where *a*, *b*, *c* and *d* are distances created by the intersection of column lines and thrust lines as shown in Figure 9. They describe two lines, one, Lf_1, extends from the center of the dome to the intersection of the thrust-lines within the HP. The other line, Lf_2, extends from that intersection point to the center of the supporting

columns. These lines, Lf_1 and Lf_2, will intersect at an angle β_{FL} For all regular layouts (rectangular, equilateral triangular and hexagonal layouts), the angle β_{FL} is equal to 90°. For irregular column arrangements, however, this angle may differ from the orthogonal value of 90°. For these non-orthogonal fall lines, the SMA equations would have to be modified to deal with non-symmetrical shapes. To circumvent this, as a modest, first approximation, the component Lf_1 is rotated around its intersection with the Lf_2 lines until β_{FL} becomes 90^o as shown in Figure 10. At the same time the components *a* and *b* of Lf_1 are multiplied by the factor cos (β - 90^o) to become a' and b'. The effect of this is that the total area defined by the height of the triangle Lf_1 and the base of Lf_2 remains unchanged, but the skewed, unsymmetrical, elliptical contour lines that would have developed, convert to the very important, symmetrical contour lines.

With the adjustment in the angle β the moment fields change to symmetrical ellipses, symmetrical hyperbolic paraboloids and symmetrical elliptical, logarithmic funnels. This modification establishes the base for the SMA. Based upon this symmetry, it confirms the original assumption of the zero value for the variables M_{xy}, M_{yx}, V_{xy} and V_{yx}. This has the further consequence that the resulting moments along the local axis are principal unit moments and as such may be expressed in the forms used in this paper. M = H*e. It also establishes the base for converting these unit moments to the resulting total moment vectors by the simple multiplication of these by the SM unit components as shown later in this paper.

Illustrative symmetrical geometries are shown in Figures 4 through 6 in which regions are basic symmetrical domains. The slab is divided into regions where each consists of one of the three basic symmetrical moment-fields shown as ED, HP and LF. Figures 7a through 7c show these developed for symmetrical square, triangular and hexagonal layouts. Eventually these are used to calculate the fixed-end-moments. The magnitude of the moments depends on the uniform load, the shape of the locally identified moment field and the relative location of the supporting columns. As will be shown later in this paper, these calculations can be made for both regular and irregular layouts (See Figure 7d).

There is a similarity in the development of the various moment fields to the "column-strip" and "middle-strip" assumptions in the ACI-318 Equivalent Frame Method. This is particularly evident in a square layout, which has been shown in Figure 7a. It should be noted, however, that in the SMA the SM shapes provide more accurate definitions, especially for the column strip bending moments.

The similarity can be summed up as follows: The elliptical dome describes the moments within two intersecting middle strips. The logarithmic funnel represents the moment in two intersecting column-strips and correctly introduces the peak moments at the columns. The hyperbolic paraboloid properly describes the moment distribution at the intersection of middle strips and column strips as these units form the symmetrical, three-dimensional moment field typical for the transition between domes and funnels. The interaction between these areas is shown in Figure 10.

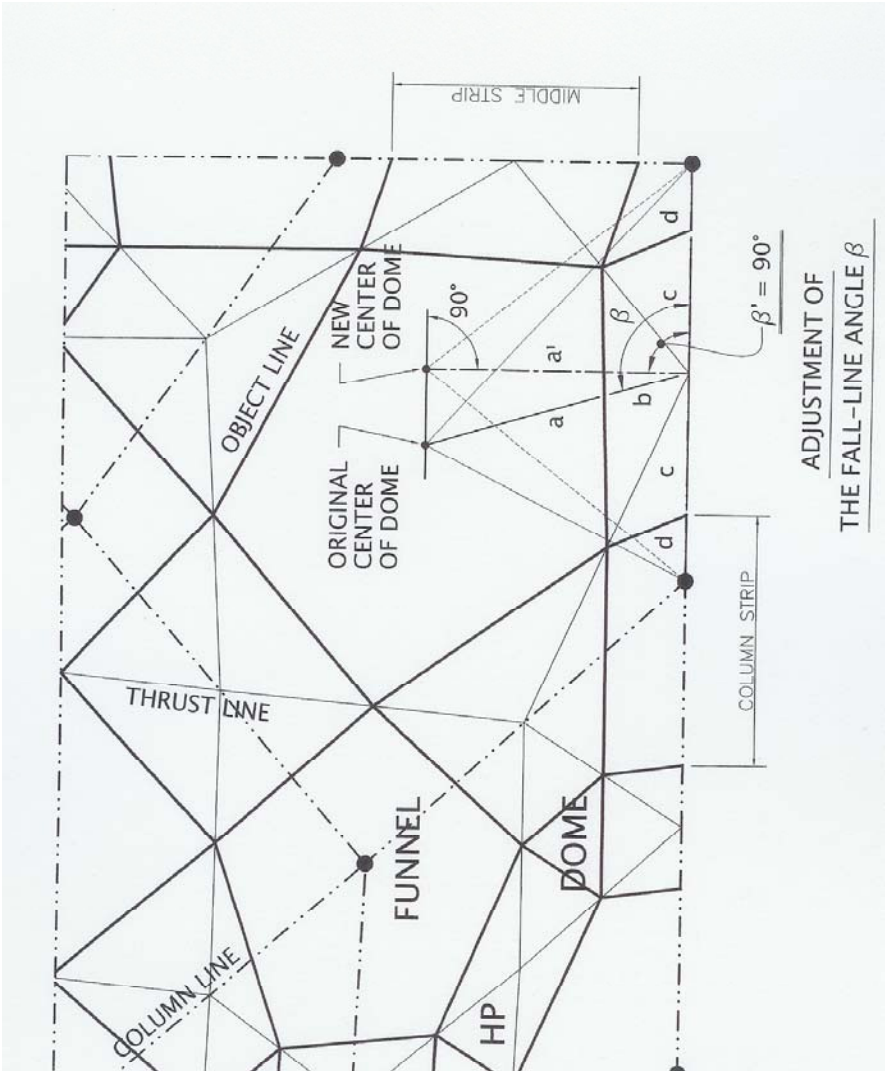

Figure 10. Division into moment fields.

Once the SM shapes have been identified, the entire slab design is obtained by applying the general equations developed by Saether (1995). These equations satisfy all equilibrium and continuity requirements between the various adjacent SM units. The superscripts D, F and HP refer to domes, funnels and hyperbolic paraboloids, respectively. The geometry of a local assemblage of SM shapes and the corresponding fall-line parameters *a*, *b*, *c* and *d* are referred to as the Structural Membrane Basic Element (SMBE) and is depicted in Figure 9. These parameters are used to calculate the basic relationships of the SMA and are defined in the following subsection.

The span from one column along the valley HP to the next column is given by:

$$L^{HP/F} = (c_1 + d_1) + (c_2 + d_2) \tag{6}$$

$c_1 + d_1$ is the distance from center of the HP to center of one column and $c_2 + d_2$ is the distance from the same HP center to the center of the opposite column as shown in Figure 7.

The span between the center of one valley HP across the dome to the adjacent valley HP is given by:

$$L^{D/HP} = (a_1 + b_1) + (a_2 + b_2) \tag{7}$$

a_1 and b_1 extend from the center of the dome to the center of the supporting HP and $a_2 + b_2$ extend from the same dome to the center of the opposite HP. This is shown in Figure 7. For symmetrical layouts these spans are:

$$L^{D/HP} = 2(a + b) \tag{8}$$

$$L^{HP/F} = 2(c + d) \tag{9}$$

In arriving at these expressions, full use is made of the similarity between the SM shapes, and the bending moments in the corresponding flat plate. To begin analyzing a layout using the SM models, the dome height h^D of the first unit is arbitrarily selected by the engineer. All other values within the same SM unit are relative to this value when calculated by using the presented SMA formulas.

The ratio of a/b is referred to as $n^{D/HP}$. From the requirement of full continuity from one SM unit to the next with regards to location, slope and loads at their common edges, the ratio of the dome height h^D to the depth of the opposing arch in the hyperbolic paraboloids, h^{HP} is referred to as $n^{D/HP}$ and is equal to:

$$\frac{h^D}{h^{HP}} = \frac{a}{b} = n^{D/HP} \tag{10}$$

From the equilibrium requirements to the exterior uniform load q and by assuming that for any dome the exterior load is divided equally in any two orthogonal directions, the following formulas are derived:

The thrust $H^{D}{}_1$ in the dome is:

$$\mathrm{H_1^D} = \frac{\mathrm{qa^2}}{\mathrm{4h^D}} \tag{11}$$

The depth of the hyperbolic paraboloid h^{HP} is:

$$h^{HP} = \frac{h^{D}}{n^{D/HP}} \tag{12}$$

In order to balance the exterior load *q,* the thrust across the HP is found to be:

$$H_1^{HP} = H_1^{D} \tag{13}$$

This thrust generates a downward reaction q_1^{HP} within the HP of the magnitude:

$$\mathrm{q_1^{HP}} = \frac{\mathrm{H_1^{HP} \cdot h^{D} \cdot 2}}{\mathrm{(b)^2 n^{D/HP}}} = \frac{\mathrm{2H_1^{HP} h^{HP}}}{\mathrm{b^2}} \tag{14}$$

The orthogonal thrust H_2^{HP} in the HP must carry this load in addition to the given uniform load w_q and is:

$$\mathrm{H_2^{HP} = H_1^{F} = \frac{(q_1^{HP} + q) \cdot (c)^2}{2h^{HP}}} \tag{15}$$

The funnel is matched to the low edge of the HP by the addition of triangular segments of inverted domes. The thrust at the low edge of the HP is the same as the thrust H_1^F along the upper rim of these funnel segments

The outline of the total contributory area, A_{TL}, carried by any one column, is identified by connecting the surrounding domes with straight lines through the HP centers and is shown in Figure 10. The total load on a column is calculated as:

$$\mathrm{W_{TL} = qA_{TL}} \tag{16}$$

From this the required thrust H_2^F along the rim of the circular funnel below the inverted dome elements, is determined as:

$$\mathrm{H_2^F = \frac{q(A_{TL} - \pi d^2)c}{4\pi dh^{HP}}} \tag{17}$$

where *c* and *d* are the fall-liner parameters as defined earlier. (See figure 9). The ratio of these two thrust values, H_1^F and H_2^F, one along the rim of the circular funnel, H_1^F, and the other along the top of the invert domes, H_2^F, is given by the following expression:

$$RN = \frac{H_2^F}{H_1^F} = \frac{(A_{TL} - \pi d^2)}{2c\,\pi d(w_1^{HP/W} + 1)} \tag{18}$$

where H_1^F is the thrust along the common border with the HP and H_2^F is the radial thrust at the funnel rim. The value of *RN* is always larger than unity, and can be calculated for any structural membrane layout.

If the horizontal thrust for circular funnels is specified to be a constant, the corresponding differential equation for the funnel shape becomes:

$$\frac{dz}{dx} = \frac{(A_{TL} - \pi x^2)q}{2\pi x H^F} \tag{19}$$

for which the solution is:

$$z = A\ln(x/d) - B(x^2 - d^2) \tag{20}$$

with:

$$A = A_{TL}w/(2\pi H^F) \;\; and \;\; B = q/(4H^F) \tag{21}$$

With the above equations the SM variable heights *e* and the horizontal thrusts *H* in all units are determined.

In the SM thin shell equivalents to the flat plate unit moments, the total required thrust is calculated along the previously identified thrust lines. The forces acting along these lines are the total forces required to maintain equilibrium between the unit stresses in the membrane shells and the exterior loads. They are the sum of the unit thrusts in the membrane, starting at the center of one dome and proceeding to the center of the other dome along the *a*-*b* fall- lines. Using the dualism between the membrane configurations and the flat plat bending moments it is now possible to convert back to the plate bending moments by using the equations:

$$M_x = H_x * e \;\; \text{and} \;\; M_y = H_y * e \tag{22}$$

With the thrust *H* known in the principal moments direction throughout the membrane and knowing that *e* is the height of the membrane, the principal unit bending moments, *M*, are known for the entire plate.

If these moments, however, are not unit fixed-end-moments, they must be modified as shown in the following. To do so it is convenient to borrow the terms “column-strip” and “middle-strip” from flat plate designs (See Figure 7d). Assuming that these strips are prismatic, and by using average moments in the funnel area, a longitudinal section cut

along the center-line of the column strip and one at center-line of the middle strip, positive and negative moment areas must add up to zero. For "Fixed-end-moments" there must be no rotation at the column supports. In the SMA, the column-strip and the middle-strip moments are analyzed independently. In other words, to arrive at the fixed-end-moments, these initial moment-areas must be added up and set equal to zero by the addition of two uniform moments: ΔM_{ms} for the middle strip and ΔM_{cs} for the column strip. These are given by the Equations 23 and 24 for the middle strip and the column strip, respectively.

$$\Delta M_{ms} = -\frac{2}{3}\frac{(M_1^D a + M_1^{HP} b)}{(a+b)} \tag{23}$$

$$\Delta \mathrm{M}_{CS} = -\frac{\frac{2}{3}(M_2^{HP} c) + M_{avg}^{1-1} R\, c}{c+d} - \frac{(\frac{1}{6} M_{avg}^{1-1} + \frac{2}{3} M_{avg}^{2-2})(d - R_c)}{c+d} \tag{24}$$

The results represent the fixed-end-moments for the slab subjected to the given loading.

In Saether (1994), the determination of the overall fixed-end moments (FEM) in the plate is described. In the present paper the calculations of the final moments in the plate in unconstrained elastic equilibrium are developed by application of a surface oriented moment-distribution.

Moment Distribution in Two-Dimensional rigid frames

For two-dimensional rigid frames, with fixed-end-moments determined for any particular layout, final moments may be determined by a one-dimensional moment distribution. This is a simple procedure developed by Croscysky and Hardy Cross (1949). For 3-D structures, such as the ones developed in the SMA, a surface oriented moment distribution has been developed. Before developing his surface oriented moment distribution in a three-dimensional structure, the basic steps of the one-dimensional moment distribution in a two-dimensional structure will be shown.

In rigid frames the moment distribution consists of three steps. The first step calculates the fixed-end-moments for any giving loading and frame geometry. This establishes the moments as statically determined units assuming all supports to be fixed. The second step is to release the fixity at each column, one column at a time. As this takes place, the juncture between each column and the attached beams will undergo a rotation corresponding to the amount of unbalanced moments resulting from the initial fixed-end condition. Free to rotate, the unbalanced moment is brought into equilibrium by small moments developing relative to their stiffness in the connected components at this time

assumed fixed at their far ends. The sum of these new moments will match the unbalanced moments and will establish equilibrium at the slab juncture, now assumed fixed in its new position. (See diagram in Figure 14a).

The rotation of a member at any one juncture will cause small moments to be generated at the far ends of these members, which remain fixed at this stage. These carry-over moments are calculated for each juncture as a third step. This results in a series of new unbalanced fixed-end-moments, located in the slabs at the various column supports. Additional iterations are necessary using the same three steps to obtain a stationary converged value. Initially, the newly generated secondary fixed-end-moments are summed up, these are balanced and the effects of these balanced moments are subsequently carried over to the adjacent supports.

In this algorithm each corrective step is completed for each column before the next sequence is started. Because several components are feeding carry-over moments into any slab juncture, these components must be computed and only distributed after the previous sequence has been completed for all supports. Only after these carry-over moments have been balanced and distributed can the first batch of distributed balancing moments be allowed to merge into the originally determined fixed-end-moments. In this way the correct amount of balancing at any one step is assured at any one completed iteration. A flowchart in Figure 14b illustrates the iteration procedure.

Moment Distribution in Flat Plates.

The surface oriented moment distribution in a 3-D flat plate system follows the same steps as outlined above for 2-D frames. Certain assumptions are required, as shown in the following. From the symmetry in the layouts it can be concluded that the assumption of an equally divided load in the two fall-line directions is accurate for square, equilateral triangular and hexagonal layouts. Similarly, a prismatic profile assumed for the various slab components is accurate for any rectangular layout and is assumed to be a valid approximation for most irregular layouts. One justification for these latter assumptions used in the calculations of the surface oriented moment-distribution is that they affect the final results with only a relatively small correction to the critical unit column moments.

The interaction between a flat plate and the supporting columns is complicated and has been the subject of numerous studies such as Corley (1961). Because of the known cracking and yielding that takes place in the slab next to the columns caused by the peak moments at these locations, an exact prediction of the relative stiffness cannot be made. As the slab cracks and the reinforcing steel yields, the slab stiffness and its rotation undergo changes that are hard to predict. Therefore, in the stiffness analysis, the assumption is made that an average modified width exists in the slab and that the column height is modified to allow for the softened slab.

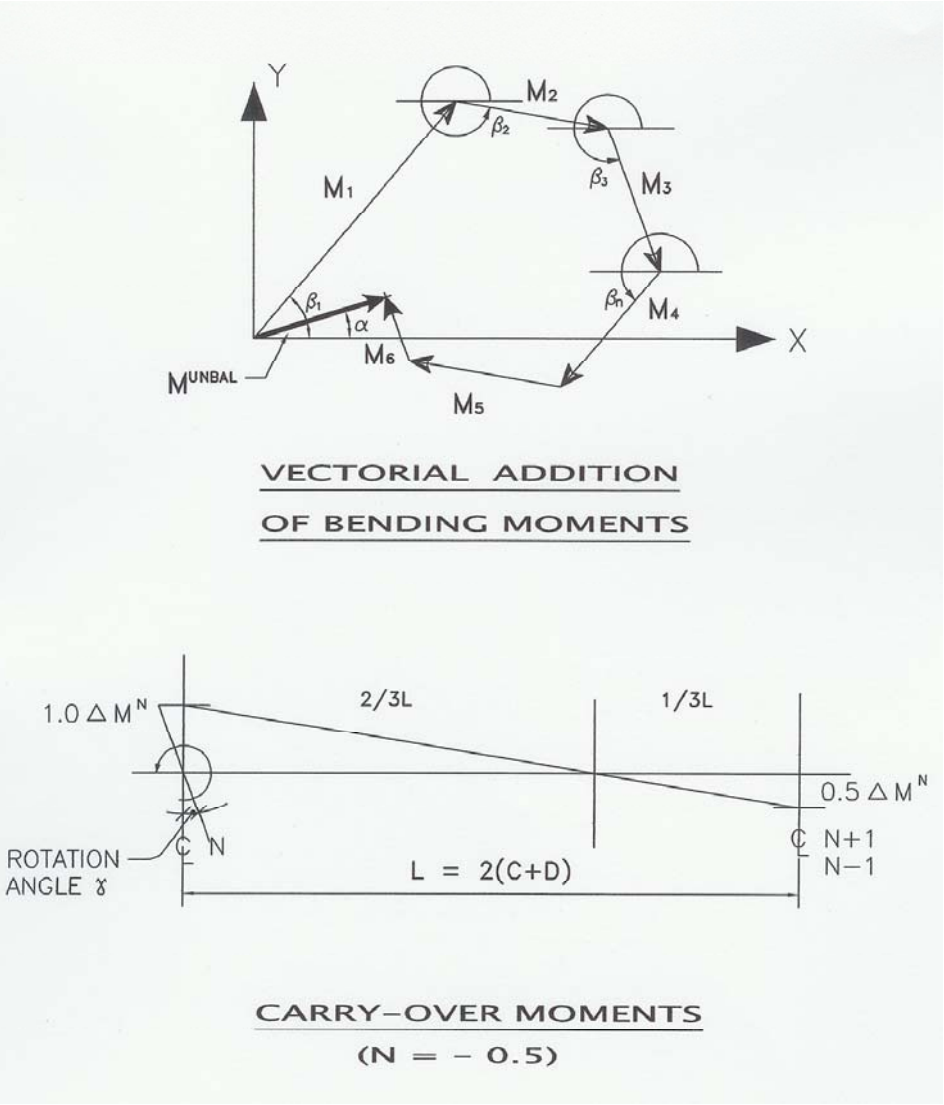

Figure 11. Basis for moment distribution.

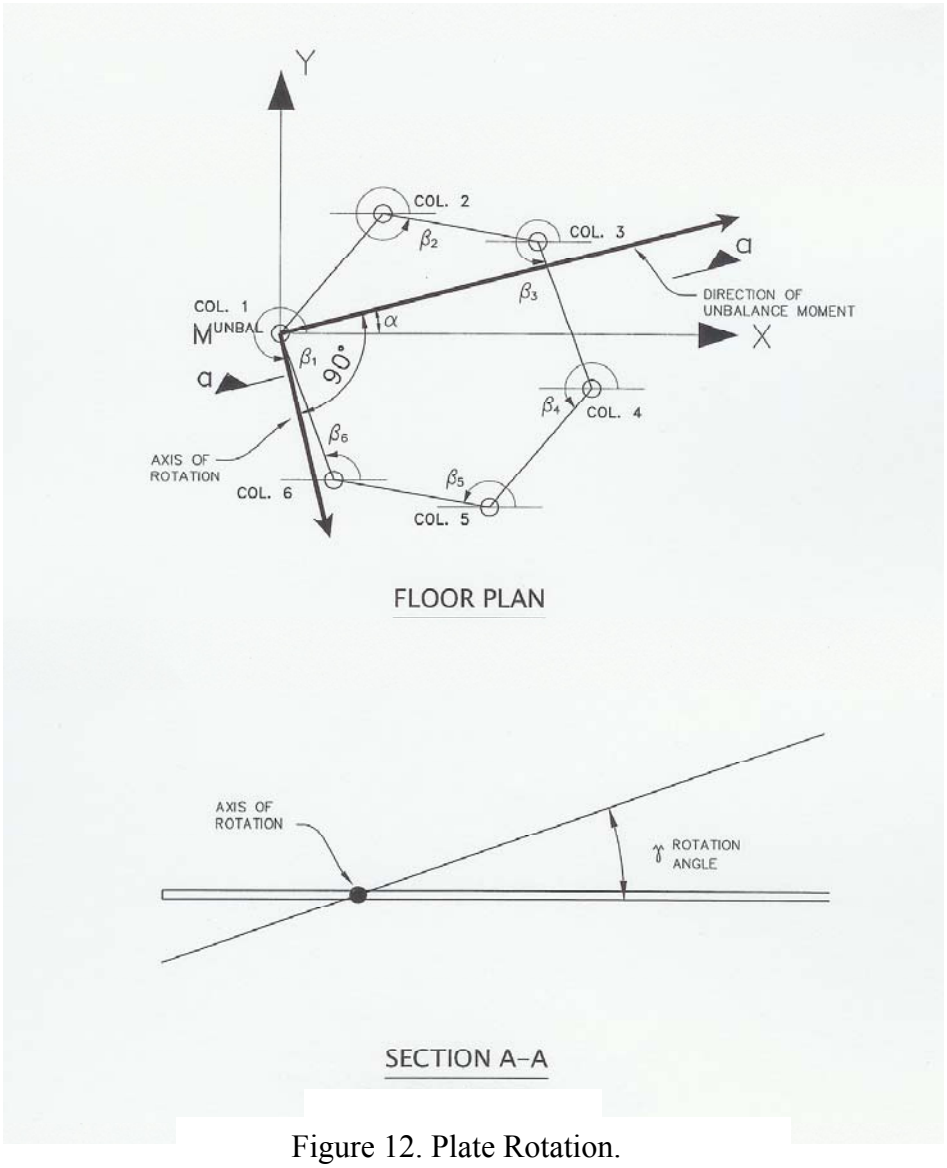

Figure 12. Plate Rotation.

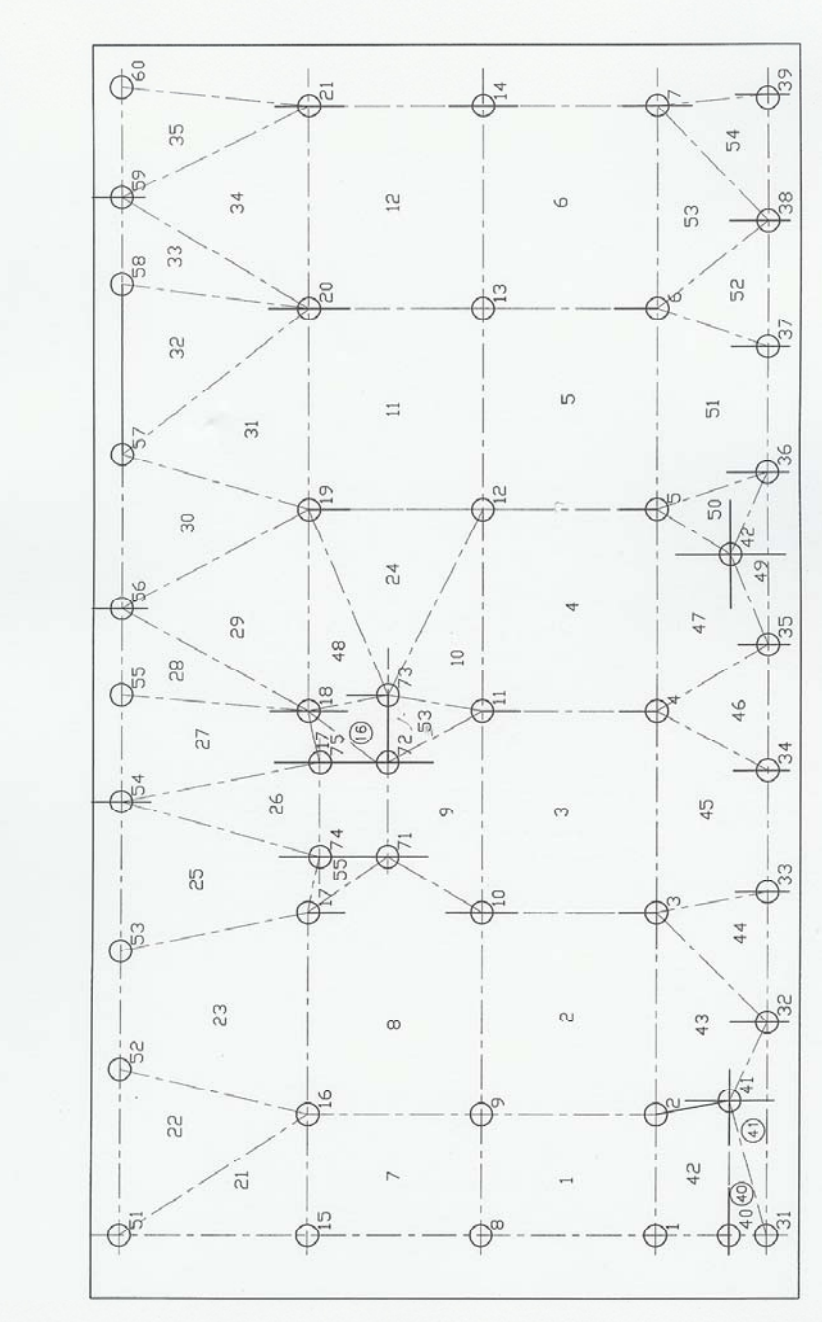

Figure 13. Typical floor plan with irregular column arrangement.

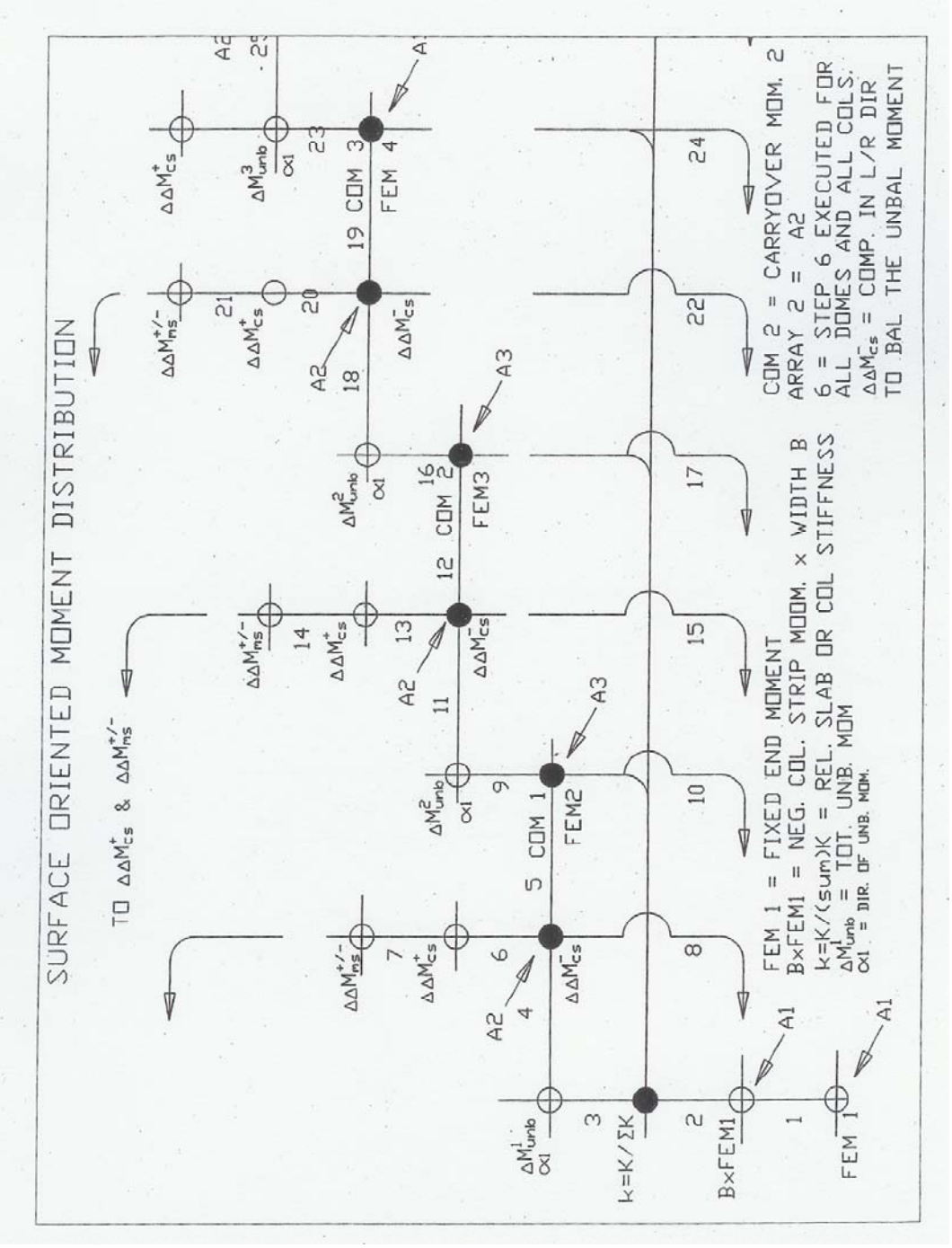

Figure 14a. Diagram of surface oriented moment distribution.

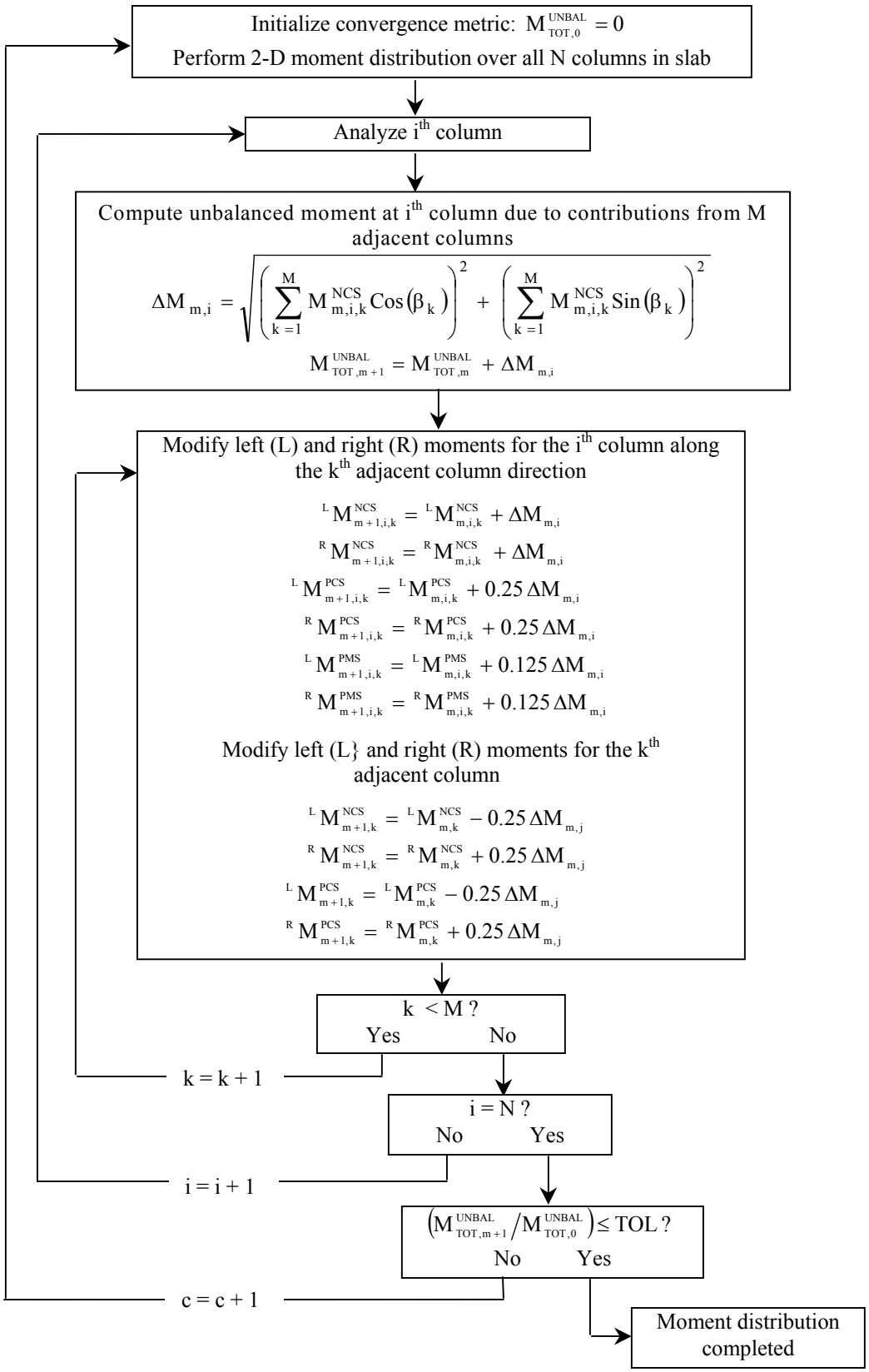

Figure 14b. Flow chart of surface oriented moment distribution.

A detailed description of the moment distribution in a flat place follows. Initially, at each column the unit fixed-end-moments are multiplied with the corresponding widths *a* and *b* of the Structural Membrane Basic Element (SMBE) to form total moments. They are added vectorially to define the unbalanced moment $M_{unbal.}$ This resulting moment acts in the direction α as shown in Figure 11. For column lines with small directional differences $(\beta_{i+1}-\beta_i) < 35^\circ$, the vectorial addition is replaced with the determination of the principal moments as explained in the previous SMA analysis section.

By removing the fixity at the columns one at the time, the slab will rotate at the column with the result that corrective moments, ΔM, will develop in the slab and column components at each column location. The magnitude of these corrective moments is a function of the unbalanced moment, M_{unbal}. The relative stiffness and the relative direction of the components involved are explained below.

The unbalanced moment at any one column *n* is the sum of the individual negative fixed-end-moments at this column which is calculated as:

$$M_{unbal} = \sum_{1}^{i} FEM_{cs}^{i} . \tag{25}$$

As the column is free to rotate, the plate /column juncture rotates around an axis in the global x-y plane at an angle α with regards to the global x-axis (See Figure 12). The angular rotation of the slab around this axis is of the magnitude γ and is the result of a balance generated by delta moments ΔM_{effe}^{n} building up in each of the connected elements of the slab and columns.

In the calculation of the relative member stiffness, it is judged to be sufficiently accurate to use the SMA factor *b* for the effective slab widths, and to use the ACI-318 equivalent column for the stiffness of the columns. For columns that are rotated in the x-y plane by an angle β_c the equation for the moment of inertia is given by:

$$I_\alpha = \frac{I_1+I_2}{2} + \frac{I_1-I_2}{2}\cos^2(\beta_c - \alpha) \tag{26}$$

where I_1 and I_2 are the principal moments of inertia in the *x* and *y* directions of the columns, β_c is the column orientation, and α is the direction of the unbalanced moment (See Figure 11).

After the relative stiffness have calculated as shown later in this chapter, the details of the moment balancing and the surface oriented moment distribution can be carried out. Initially, all fixed-end-moment are multiplied by their contributory widths *a'* and *b'*, and added vectorially. For small β angle differences, the pairs of unit moments are replaced by their principal moments as described above.

The resulting unbalanced moments, M_{unbal}, acting in directions α as shown in Figure 11 are obtained. These unbalanced moments are distributed to the various slab components along the column lines and to the corresponding columns according to their relative stiffness.

In the relative stiffness calculations for the slab, it is assumed that the moments of the entire width $a + b$ of the column and the middle strips would apply, but that the stiffness of the column strip b alone would determine the stiffness of this component. This assumption would balance all end moments from column and middle strips, but only the stiffness of the column strip would be used in determining the relative stiffness of this part of the slab.

With the relative stiffness of each slab member established, the actual moments are found to be:

$$\Delta M^{j}_{act} = k^{j}_{n,m}\, M_{unbal} \cos(\beta - \alpha) \tag{27}$$

The effective distributed moments are moments caused by the rotation of the plate and column at column n. They are equal to the actual change in distributed moments, ΔM^{i}_{act}, times the factor $cos(\beta-\alpha)$. But these are the moment ΔM^{i}_{max} times the factor $cos(\beta-\alpha)$. The effective moment is therefore given by:

$$\Delta M^{I}_{eff} = \cos^2(\beta - \alpha)\, M^{i}_{max} \tag{28}$$

In these expressions α is the rotation angle explained above and β is the direction of each column line. These actual moments ΔM^{i}_{act} are the unbalanced moment times the relative stiffness of each slab and column element at this juncture. The effective moments can be expressed as follows:

$$\Delta M^{i}_{eff} = k^{i}_{rel,eff}\, M_{unbal} \tag{29}$$

where $k^{i}_{rel,eff}$ it given by:

$$k^{i}_{rel,eff} = \cos^2(\beta - \alpha)\, K^{i} \sum_{i=1}^{j} K^{i} \tag{30}$$

The expressions K^i are the stiffness of each member meeting at any one slab/column juncture.

Each column/slab juncture is balanced through the process of assuming incremental free rotation in which all other junctures are assumed fixed. The result is that while one

juncture rotates, the far ends of the connected members are subjected to what is referred to as 'carry-over-moments'. Besides affecting the moments at the neighboring column locations, eventually all slab areas are affected by a series of small moment changes. They amount to given fractions of the balanced moments ΔM_{act}^{i} as described later in this paper.

At this point it is necessary to stress that the initial moment balancing must be completed and independently stored for all columns before the 'carry-over-moment' calculations are started, and that the 'carry-over-moments' must be calculated and independently stored before any moment adjustment can take place in the slab/column framing members.

The above algorithm distributes moments from each column to the adjacent columns at each step. Therefore, iterations must be repeatedly performed to communicate updated moments over the entire slab. For each iteration, the amount of correction is greatly reduced due to rapid convergence. The process is continued until the total correction is less than a preset lower limit.

A summary of the formulas developed for the surface oriented moment distribution are presented below.

The relative effective stiffness of the slab components is computed as:

$$k_{n,m} = \cos^2(\beta - \alpha) K_{n,m} / \sum_{i}^{m} K_{n,m} \cos^2(\beta - \alpha) \tag{31}$$

K_n is the stiffness of the various slab and column units, and $\cos^2(\beta-\alpha)$ is a stiffness reduction factor due to the relative position of the column line with regards to the direction of the rotation of the slab as shown later in this chapter.

The stiffness of the slab components and the columns are given below.

For the slab components it is:

$$K_{slab} = \frac{b}{24} \frac{t^3}{(c+d)} \tag{32}$$

For the columns it is:

$$K_{col} = \frac{Wd^3}{12h_c} \tag{33}$$

where b, c and d are the structural membrane basic element (*SMBE)* parameters and h_c is the column height below and above the slab. W and d are the width and depth of the column, respectively.

In these calculations, where β is the direction of the various resistive slab components as given by the slab column lines, and α is the direction of the unbalanced moment rotation, each slab component forms an angle $(\beta-\alpha)$ with the direction of the unbalanced moment as shown in Figure (11). As the slab rotates by the amount γ_{max} in the direction of α at any one column, each component within the slab rotates by a magnitude of γ_{max} reduced by the factor $cos\ (\beta-\alpha)$. The rotation of any of the connected members within the plate is therefore:

$$\gamma^{i} = \gamma^{i}_{max} \cos\ (\beta-\alpha) \tag{34}$$

Furthermore, the effective moment, ΔM_{effe}, in resisting the unbalanced moment, M_{unbal}, is the actual moment component, ΔM^{n}_{act}, reduced by a similar factor $cos\ (\beta - \alpha)$. This allows for the fact that if the angle $(\beta-\alpha) = 0$, the moment component is in direct line with the unbalanced moment, M_{unbal}, and therefore is resisting this rotation with an unreduced value. Similarly, if the angle $(\beta-\alpha) = 90^{o}$, the moment is normal to the rotation and, by ignoring any torsional resistance, would have no effect in resisting the unbalanced moment as shown in Figure 12. As a result, the effective component of the moment, $\Delta M^{n}_{eff.}$, resisting the rotation, γ, is the actual moment, $\Delta M^{n}_{act.}$, multiplied by the factor $\cos(\beta-\alpha)$ which may be expressed as:

$$\Delta M^{n,m}_{eff} = k_n\ M_{unbal} \cos^{2} (\beta-\alpha) \tag{35}$$

or by expressing the effective relative stiffness k at any one column *n* in any column line direction *m.* This relative stiffness can be expressed as follows:

$$k^{n,m}_{effe} = k^{n,m}_{i} \cos^{2} (\beta-\alpha) \tag{36}$$

Because the total sum of the effective moments must be equal to the total sum of the unbalanced moment, it is

$$\sum_{1}^{m} \Delta M_{eff} = \sum_{1}^{m} M^{n,m}_{fem} \tag{37}$$

and because the total sum of the newly established delta fixed-end-moments by definition is equal to the unbalance moment, M_{unbal}, the effective resisting moment is:

$$\Delta M^{n,m}_{eff} = k^{n,m}_{effe}\ M_{unbal} \tag{38}$$

In order to obtain the actual bending moments in the moment distribution, the following relation applies:

$$\Delta M^{n,m}_{act} = \Delta M^{n,m}_{eff} / \cos\ (\beta-\alpha) \tag{39}$$

The bending moment change, *ΔM*, resulting from the moment distribution at column n generate the following 'carry-over-moments', *ΔΔM,* in the adjoining columns and slab areas:

In the negative column strip:

$$\Delta\Delta M_{cs}^{n,m} = (-0.5)\,\Delta M_{act}^{n,m} \tag{40}$$

In the positive column strip:

$$\Delta\Delta M_{cs}^{n,m} = (+0.25)\,\Delta M_{act}^{n,m} \tag{41}$$

In the negative middle strip:

$$\Delta\Delta M_{ms}^{n,m} = (-0.125)\,\Delta M_{act}^{n,m} \tag{42}$$

In the positive middle strip:

$$\Delta\Delta M_{ms}^{n,m} = (+0.125)\,\Delta M_{act}^{n,m} \tag{43}$$

The factors +/- 0.125 used for the moment corrections in the middle strip are linear approximations of these moments and are judged to be satisfactory for these small plate moments. The + 0.25 factor used for the positive column moment at mid-span is a direct result of the carry-over-moments along the column lines.

As the balancing moments, *ΔM*, and the carry-over-moments, *ΔΔM*, are being generated, these generated moments must be stored temporarily until all columns have been balanced. At this point the original negative fixed-end-moments, M_{init}^{n}, together with the various field moments are modified. The initial surface oriented moment distribution balances the fixed-end-moments in the negative column strip, but the following carry-over-moment distribution of the first iteration creates new unbalanced moments in the column strip and the middle strip.

The new negative column strip moment is given by:

$$M_{fem}^{n,m} = M_{init}^{n,m} + \Delta M_{act}^{n,m} + \Delta\Delta M_{cs}^{n,m} \tag{44}$$

This new positive column strip moment is given by:

$$M_{cs+}^{n,m} = M_{init+}^{n,m} + \Delta\Delta M_{cs+}^{n,m} \tag{45}$$

The new negative middle strip moments are given by:

$$M_{ms-}^{n,m} = M_{init-t}^{n,m} + \Delta\Delta M_{ms-}^{n,m} \quad (46)$$

The new positive middle strip moments are given by:

$$M_{ms+}^{n,m} = M_{init+}^{n,m} + \Delta\Delta M_{ms+}^{n,m} \quad (47)$$

Subsequent iterations must then be carried out until the total sum of changes in the negative column strip moments is below a given tolerance.

As moment balancing takes place, the column loads in the affected columns are corrected to correspond to the adjustments in the slab bending moments at these columns. This correction is:

$$\Delta P = \frac{\Delta M_{act.}}{2(c+d)} \quad (48)$$

The values of *c* and *d* are the values obtained from the SMBE as shown in Figure 9.

The described approach determines the final moments in the plate. Of controlling importance are the negative moments at the column supports. In the SMA analysis these moments are given with their maximum peak values as well as averaged values allowing for cracking of the concrete and yielding of the reinforcing steel. It must be remembered, however, that this averaging is only allowed where the resulting concrete sections are under-reinforced.

Basically, the total resistive moment offered by any one strip radiating out from a column is the sum of the computed average negative unit moments multiplied by the corresponding slab widths *b'*, plus the negative middle strip unit moments multiplied with the width *a'* of the middle strip to produce a total resistive moment.

In an irregularly supported slab these final moments are acting along randomly oriented column lines. It is desirable, however, to obtain design moments that are acting along the selected *x* and *y* axes of the slabs in a global coordinates system. These moments may be obtained by vectorially adding these various balanced total moments. This vectorial addition is subject to the previously mentioned modifications as required by the relative orientation of the established column lines.

In computing the sums of positive and negative column components, the column- and middle-strip unit moments are multiplied by the corresponding values of *b'* and *a'*, respectively, as described above. To arrive at the average unit design moments, each sum so established is then divided by the sum of the corresponding *a'* and *b'* values. If these linear sums exceed the actual available strip widths, the sum must be limited to these available widths, while the unit moments are increased accordingly, in order to maintain the correct total moments. These increases are controlled by the factors $a_{calculTED} / a_{available}$ respective $b_{calculated} / b_{available.}$

Comparison Studies

Figure 13 shows a typical irregular column layout used in one comparison study. In this study the columns 6, 12, 13, and 14 have been selected to show a comparison between the column strip moments M_x and M_y predicted by SMA and the popular finite element design code ETABS (2002). Four columns were selected as representing some of the typical conditions that exist in this particular design. The comparison involve the average and the maximum moments in the x and y directions at the face of the selected columns. Whereas these values are explicit outputs in the SMA, in the ETABS output the same values had to be extracted from contour plots. A simple interpolation and integration scheme was used with the ETABS graphical output to obtain average moments. Important similarities and differences were evident. As can be deducted from table 1, the general agreement was quite good. In a total of four columns with 16 items of comparison, one of the ETABS items gave illogical results. This was the column strip moments normal to the edge of one edge column.

TABLE1.

Comparison between SMA and ETABS Bending Moments.

M_x max.		`		M_y max.	
COLUMN	SMA	ETABS	COLUMN	SMA	ETABS
12	42.0	39.5	12	45.0	33.0
13	15.0	16.0	13	42.5	37.5
14	45.0	45.0	14	34.5	24.5
6	36.0	32.0	6	35.0	36.0
M_x ave.		`		M_y ave.	
COLUMN	SMA	ETABS	COLUMN	SMA	ETABS
12	16.4	18.2	12	16.0	14.5
13	20.0	23.5	13	45.0	44.0
14	7.0	NA	14	15.0	12.0
6	13.0	17.0	6	13.0	13.0

The comparison shows a close similarity between the two sets of values. The SMA, however, is yielding results with a minimum of calculations yet avoiding the convergence

difficulties and lengthy run-times generally required in the ETABS finite element-based approach.

Summary

A general flat plate analysis has been presented using a development referred to as the Structural Membrane Approach (SMA). This approach is based on a unique structural model which allowed slab moments to be represented as a combination of three basic 3-D functions for local moment fields. These functions are referred to as Structural Membrane shapes and express a dualism between plate bending moments and the displacement patterns of stretched elastic membranes subjected to lateral loads.

The original formulation of SMA focused on the determination of the fixed-end-moments in flat plate designs. The present paper extends the capabilities of the SMA by developing a moment balancing procedure between different areas and supports by utilizing a surface oriented moment distribution. This approach resulted in an extremely efficient, intuitive and useful methodology for analyzing regular and irregular slab layouts.

Notation

A	=	size of slab area
a	=	fall line parameters in the SMT
b	=	fall line parameters in the SMT
c	=	fall line parameters in the SMT
d	=	fall line parameters in the SMT
d	=	depth of column
E	=	Young's Modulus of elasticity
e	=	depth of shell
H	=	thrust in the shell
h_1^D	=	dome height
h^{HP}	=	height of hyperbolic paraboloid
h_c	=	height of column
I	=	moment of inertia
K	=	total stiffness
k	=	relative stiffness
l	=	span length
M_{act}	=	actual moment (in line with the slab component)
M_{eff}	=	effective moment (in line with and resisting the unbalanced moment)
M	=	slab moment
M_x	=	moment in x – direction
M_y	=	moment in y – direction
ΔM	=	change in moment

$M_{fem}^{n,m}$ = FEM at column *n* in *m* direction

$\sum_{1}^{m} M_{fem}^{n,m}$ = sum from *1* to *m* of FEM at column *n*

$\Delta M_{act}^{n,m}$ = distributed moment at column *n* in *m* direction

$\Delta M_{eff}^{n,m}$ = effective distributed moment at column *n* in α direction from distributed moment in *m* direction

$\sum_{1}^{M} M_{eff}^{n,m}$ = sum of effective distributed moments at column *n*

$K^{n,m}$ = stiffness of member *m* at column *n*

$\sum K^{n}$ = sum of member stiffness at column *n*

$k^{n,m}$ = relative stiffness of member *m* at column *n*

$k_{eff}^{n,m}$ = effective relative stiffness of member *m* at column *n*

$\Delta\Delta M_{act}^{+cs.n}$ = correction of column strip positive moment at column line *n-m* in direction of column *m* due to carry-over-moment at column line *n-m*

$\Delta\Delta M_{act}^{-msn}$ = correction in middle strip negative moment at and normal to column line *n-m* due to carry-over-moment form column *n* to column *m*

$\Delta\Delta M_{act}^{+msn}$ = correction in positive field moments inside of column line *n-m* due to carry-over-moment from column *n* to column *m*

n = SMT parameter

q = uniform load

t = slab thickness

w = width of column

α = direction of slab rotation

β = direction of column line

γ = slab rotation with rotation axis in the *x-y* plan

β_{FL} = direction of fall line

References

1. Timoschenko, S., and Woinowsky-Krieger, S., Theory of plates and shells, McGraw-Hill Book Co., New York, N.Y., 1959.
2. Saether, K., "The Structural Membrane," ACI Journal, Title No. 57-41, pp. 827-850, 1961.
3. Saether, K., "Flat plates with regular and irregular column layouts, I Analysis & II Numerical evaluation," ASCE Journal, Vol. 120 (5), 1994.
4. Saether, K., "Structural membrane shells," International Association for Shells and Special Structures. International Symposium, Milan, Italy, 1995.
5. Park, R., and Gamble, W.L., Reinforced concrete slabs, 2nd edition, New York, Wiley, 2000.
6. Hardy, C., "Analysis of Continuous Frames by Distributing Fixed-End-Moments," L.B. Grinler. New York, 1949.

7. Corley, J. and Jirsa, J. “The equivalent frame analysis for reinforced concrete slabs,” Dept. of Civil. Engineering, University of Illinois, Urbana, Illinois, 1961.
8. Etabs, Computers and Structures, Inc., Berkeley, California, 2002.
9. Baskaran, K., “Flexural behaviour of reinforced concrete slabs supported on non-rectangular column grid,” PhD Dissertation, University of Cambridge, UK, 2004.
10. Markus, H., Die Theorie elasitscher Gewebe und ihre Anwendung auf die Berechnung biegsamer Platten, verlag von Julius Springer, Berlin, 1924.
11. Hillerborg, A., Strip Method Design Handbook, E & FN Spon, 1996.
12. DenHartog, J. P., Advanced Strength of Materials, McGraw-Hill, New York 1952